Analysis of Errors Due to Polynomial Adjustment of Altimeter Profiles

P. Y. LE TRAON,* C. BOISSIER** AND P. GASPAR*

(Manuscript received 10 August 1990, in final form 20 November 1990)

ABSTRACT

Among the various sources of error on altimetric sea surface height variability, the orbit error has the largest amplitude. However, since orbit error is mostly at long wavelengths, it can theoretically be distinguished from the mesoscale signal, characterized by wavelengths of a few hundred kilometers. The most commonly used technique to subtract this long-wavelength error is polynomial adjustment (zero, first or second degree) over distances of a few thousand kilometers. This paper examines the error on estimating the polynomial, which directly impacts the mesoscale signal obtained after the adjustment. We demonstrate how it can be estimated in theory and how it varies according to the spatial and energetic mesoscale characteristics (variability level, nonhomogeneities). These results are checked against simulated data and validated using actual Geosat data. The error is far from negligible: for a first-degree fit over 1500 km or a second-degree fit over 2500 km, its amplitude is typically 30% to 50% of the total mesoscale signal amplitude at the profile center and ends, respectively. In certain cases, where nonhomogeneity is significant, it can be greater than the total signal amplitude. We show that in such cases, a polynomial adjustment that takes account of the statistics of mesoscale signal is a considerably better method. However, in the longer term, more global techniques such as inverse methods should be used so that the mesoscale signal can be extracted with the fewest possible errors.

1. Introduction

Of the various sources of error on altimetric measurements of surface topography, the largest is orbit error, caused by imperfect knowledge of the spacecraft position, and uncertainty on the geoid. As the geoid signal is stationary at the time scales under consideration (roughly a few months), geoid errors can be eliminated for studies of the oceanic mesoscale variability. Orbit error is generally characterized by a long wavelength (about 40 000 km) and can theoretically be distinguished from the mesoscale ocean signal, which has characteristic wavelengths around a few hundred kilometers. Polynomial adjustment (degrees 0, 1 or 2) is the most common of the various procedures to subtract this long-wavelength error for distances on the order of 10^3 km. This adjustment is supposed to provide the best representation of orbit error on the fraction of arc under consideration. Tai (1989) estimated the residual orbit error after adjustment, assuming a sine wave orbit error with a period of one cycle per revolution. Rosborough and Marshall (1990) have complemented this approach, using a more realistic orbit error spectrum. The two studies show that for polynomial adjustments, which are generally used to extract the mesoscale signal (e.g., Cheney et al. 1983; Le Traon et al. 1990; Zlotnicki et al. 1989), the residual orbit error is low and usually negligible.

Error on estimation of the correction polynomial is another source of error affecting the mesoscale signal obtained after adjustment. The accuracy with which a polynomial can be estimated depends on the number of degrees of freedom, or number of independent measurements, on the arc concerned. Given the mesoscale decorrelation scales, the number of degrees of freedom may be low and errors nonnegligible. Examination of the data obtained after such polynomial adjustments, and particularly the evolution in time of an eddy field, seems to confirm this. Although these errors are not a major problem for work on a given track, they can be so for two-dimensional (x, y) or three-dimensional (x, y, t) mesoscale mapping. In such cases, the error is different from one track to the other and from one cycle to the next. Polynomial fitting errors can thus conceal, or magnify, certain structures. These errors due to polynomial adjustment were observed by Sandwell and Zhang (1989) in their analysis of Geosat data. Their results suggest that bias and tilt adjustment can cause significant artificial variability at the ends of profiles.

Although it is a fairly simple task, these errors have not yet been analyzed theoretically. This is the purpose of this paper. The main objective is to provide a diagnostic of these errors in terms of their statistics in different situations. This is not only important for data interpretation, but also for correction of the error itself. We shall also show that account should be taken of

* CLS Argos, Toulouse, France.
** SHOM, CNES/GRGS, Toulouse, France.

Corresponding author address: Dr. P. Y. Le Traon, CLS ARGOS, 18 Avenue Edouard Belin, 31055 Toulouse Cedex, France.

© 1991 American Meteorological Society

Unauthenticated | Downloaded 10/04/22 03:28 AM UTC

mesoscale statistics if a better polynomial fit for orbit errors is to be obtained.

Section 2 is an illustration of how a simple bias adjustment can affect the estimated signal. Section 3 generalizes the approach for any given functional form of adjustment. Section 4 illustrates the results obtained for the polynomial adjustments generally used. These results are verified using simulated and real data in section 5. Polynomial adjustment techniques are compared with more elaborate objective analysis methods in section 6. The conclusion in section 7 summarizes the main results of the study and their practical impact.

2. A simple example: Bias adjustment

Assume that the orbit error on the fraction of arc under consideration (here 1500 km) can be perfectly modeled by a constant a_0. Let $h(x)$ be the altimetric height once the mean profile has been subtracted. Assuming measurement errors to be zero, we obtain

$$h(x) = a_0 + h'_{\text{meso}}(x) \tag{1}$$

where h'_{meso} is the mesoscale variability signal. Its mathematical expectation (in practice, its temporal mean), denoted by $\langle h'_{\text{meso}} \rangle$, is by definition zero. For the sake of simplicity, assume here that the sampling interval is 1 point per 150 km and that the mesoscale signal is decorrelated from one measurement point to the next. We thus have 10 points per profile ($N = 10$).

To reduce the orbit error, we proceed by conventional least squares fitting, i.e., we seek ϵ_{orb} that minimizes $\sum_{i=1}^{N} [h(x_i) - \epsilon_{\text{orb}}]^2$. The solution being, obviously, the mean of the measurements, we obtain, using (1):

$$\epsilon_{\text{orb}} = a_0 + \frac{\sum_{i=1}^{N} h'_{\text{meso}}(x_i)}{N}. \tag{2}$$

The altimetric residuals $h'_{\text{est}}(x)$ obtained after removing the estimated orbit error are thus:

$$h'_{\text{est}}(x_i) = h(x_i) - \epsilon_{\text{orb}} = h'_{\text{meso}}(x_i) - \frac{\sum_{i=1}^{N} h'_{\text{meso}}(x_i)}{N} \tag{3}$$

and have an estimation error:

$$\epsilon_{\text{LSQ}} = \frac{\sum_{i=1}^{N} h'_{\text{meso}}(x_i)}{N}. \tag{4}$$

The mathematical expectation of ϵ_{LSQ}, denoted $\langle \epsilon_{\text{LSQ}} \rangle$, is zero. Its variance is

$$\langle \epsilon^2_{\text{LSQ}} \rangle = \frac{\sum_{i=1}^{N} \sigma^2(x_i)}{N^2} \tag{5}$$

where $\sigma^2(x_i)$ is the variance of the mesoscale signal, i.e., $\sigma^2(x_i) = \langle h'_{\text{meso}}(x_i)^2 \rangle$. The error, as given by (4), is constant along the profile and correlated with the signal. Indeed, using (4), one obtains

$$\langle \epsilon_{\text{LSQ}} h'_{\text{meso}}(x_i) \rangle = \frac{\sigma^2(x_i)}{N} \tag{6}$$

and therefore:

$$\langle h'_{\text{est}}(x_i) \rangle^2 = \sigma^2(x_i) + \langle \epsilon^2_{\text{LSQ}} \rangle - 2\frac{\sigma^2(x_i)}{N}. \tag{7}$$

a. *Case of homogeneous mesoscale variability*

If σ does not depend on x_i, (5) and (7) give, respectively, $\langle \epsilon^2_{\text{LSQ}} \rangle = \sigma^2/N$ and $\langle h'_{\text{est}} \rangle^2 = \sigma^2(1 - 1/N)$. It follows that, in this case, the mesoscale variability is always underestimated. In our simple example, this gives a standard deviation of the estimation error as large as 30% of the signal standard deviation and an underestimation of the mesoscale variability variance of 10%.

b. *Case of nonhomogeneous mesoscale variability*

Let us now examine the case of nonhomogeneous mesoscale variability, i.e., $\sigma = \sigma(x)$. For example, let σ be 30 cm on the first five points and 5 cm on the last five.

If we calculate the bias by conventional least-squares fitting, which does not take account of the noise statistics (here the mesoscale signal), we obtain, using (5), $\langle \epsilon^2_{\text{LSQ}} \rangle^{1/2} = 6.8$ cm, i.e., greater than the weak variability signal (5 cm). In addition, (7) yields $\langle h'_{\text{est}}(x_i)^2 \rangle^{1/2} = 27.6$ cm for the first five points and 8.1 cm for the last five points.

Now turning to weighted least-squares methods (e.g., Liebelt 1967), which take account of the different variances of the errors, the bias is obtained by minimizing $\sum_{i=1}^{N} [h(x_i) - \epsilon_{\text{orb}}]^2/\sigma(x_i)^2$, which yields:

$$\epsilon_{\text{orb}} = a_0 + \frac{\sum_{i=1}^{N} h'_{\text{meso}}(x_i)/\sigma(x_i)^2}{\sum_{i=1}^{N} 1/\sigma(x_i)^2}. \tag{8}$$

The error on $h'_{\text{meso}}(x_i)$ is thus equal to

$$\epsilon_{W\text{LSQ}} = \frac{\sum_{i=1}^{N} h'_{\text{meso}}(x_i)/\sigma(x_i)^2}{\sum_{i=1}^{N} 1/\sigma(x_i)^2}. \tag{9}$$

In our example, $\langle \epsilon^2_{W\text{LSQ}} \rangle^{1/2} = 2.2$ cm, i.e., well under the error obtained above. More weight is given to data with the weakest mesoscale signal which, for orbit error determination, is considered as noise. Once the bias has been subtracted, the remaining variabilities are much closer to the true values:

Unauthenticated | Downloaded 10/04/22 03:28 AM UTC

$$\langle \epsilon_{W\mathrm{LSQ}} h'_{\mathrm{meso}}(x_i) \rangle = \langle \epsilon^2_{W\mathrm{LSQ}} \rangle \quad (10)$$

$$\langle h'_{\mathrm{est}}(x_i)^2 \rangle = \langle h'_{\mathrm{meso}}(x_i) \rangle^2 - \langle \epsilon^2_{W\mathrm{LSQ}} \rangle. \quad (11)$$

We thus have $\langle h'_{\mathrm{est}}(x_i)^2 \rangle^{1/2} = 29.9$ cm for the first five points and 4.5 cm for the last five points.

This highly simplified example is a good illustration of the error that can occur on bias estimation from data with mesoscale-induced noise (with respect to the estimate). The mesoscale signal is correlated over long distances (a few hundred kilometers), which implies that the number of degrees of freedom on estimation of the bias is low. The value chosen for $N(10)$ represents the true number of degrees of freedom on a 1000–1500 km track. The example also shows that least-squares methods that take account of the error statistics can be very useful. We shall extend the problem to the adjustment of any function (1-, 2-, etc., degree polynomials), comparing the conventional least-squares (LSQ) method with the more elaborate technique of objective mapping by least-squares fitting (Davis 1985). This method, hereafter referred to as OM, explicitly takes into account the noise statistics.

3. Generalization

Now we assume that the orbit error can be perfectly modeled, on the fraction of arc under consideration, by a linear combination of M functions $F_m(x)$ [e.g., $F_m(x) = x^m$]:

$$\epsilon_{\mathrm{orb}}(x) = \sum_{m=1}^{M} b_m F_m(x). \quad (12)$$

Note that in the following examples (first-degree polynomials over 1500 km and second-degree over 2500 km), the modeling error is, in practice, negligible. It can be estimated at 0.25% and 0.026%, respectively, of the rms orbit error (Tai 1989). For the Geosat GDR orbit, this means errors well under a centimeter.

The sea surface height $h(x)$, after removing the mean profile, can be written under the form:

$$h(x) = \sum_{m=1}^{M} b_m F_m(x) + h'_{\mathrm{meso}}(x) + \epsilon'(x) + b_{\mathrm{alt}}(x) \quad (13)$$

where $\epsilon(x)$ is the error due to inaccuracy on correction of altimeter measurement (electromagnetic bias, troposphere, inverse barometer effect, etc.) and $b_{\mathrm{alt}}(x)$ is the altimeter measurement noise assumed to be a white noise with variance b^2.

We shall consider that the b_m also contain the $\epsilon(x)$ signal, which can be expressed in the form given in (12), i.e., the long wavelength part of the signals. The residual signal ϵ' of ϵ is weak and, for midlatitude regions, $\langle \epsilon' \rangle^2$ is typically on the order of, or less than, $0.1 \langle h'_{\mathrm{meso}} \rangle^2$ (Jourdan 1990). For the sake of simplicity, we shall disregard it in the following discussion. Thus, $h(x)$ becomes the sum of the orbit error (the signal of interest) and of the mesoscale signal and the altimetric noise (the measurement errors).

a. *Conventional least-squares method (LSF)*

The conventional method for adjusting functions by least squares consists in estimating the b_m ($m = 1, \cdots, M$) such that

$$\sum_{i=1}^{N} [h(x_i) - \sum_{m=1}^{M} b_m F_m(x_i)]^2 \text{ is minimized.} \quad (14)$$

The following solution is easily obtained:

$$b_m = B_{\mathrm{LSQ}_m} = \sum_{i=1}^{N} \sum_{k=1}^{M} Z^{-1}_{\mathrm{LSQ}_{m,k}} F_k(x_i) h(x_i) \quad (15)$$

where

$$Z_{\mathrm{LSQ}_{m,k}} = \sum_{i=1}^{N} F_m(x_i) F_k(x_i).$$

The error on B_{LSQ_m} ($\delta B_{\mathrm{LSQ}_m}$) is due to the error on h (i.e., h'_{meso} and b_{alt}), and its covariance is equal to

$$\langle \delta B_{\mathrm{LSQ}_m} \delta B_{\mathrm{LSQ}_n} \rangle = \sum_{i,j=1}^{N} \sum_{k,k'=1}^{M} Z^{-1}_{\mathrm{LSQ}_{m,k}} Z^{-1}_{\mathrm{LSQ}_{n,k'}} F_k(x_i) F_{k'}(x_j) A_{ij} \quad (16)$$

where $A_{ij} = C(x_i, x_j) + \delta_{i,j} b^2$. Here $C(x_i, x_j)$ is the spatial covariance of the mesoscale signal between x_i and x_j.

The error on estimation of $\epsilon_{\mathrm{orb}}(x) \epsilon_{\mathrm{LSQ}}$, which directly impacts the mesoscale signal after adjustment, has thus a variance given by

$$\langle \epsilon_{\mathrm{LSQ}}(x)^2 \rangle = \sum_{m,n=1}^{M} \langle \delta B_{\mathrm{LSQ}_m} \delta B_{\mathrm{LSQ}_n} \rangle F_m(x) F_n(x). \quad (17)$$

The correlation of this error with $h'_{\mathrm{meso}}(x_i)$ is

$$\langle \epsilon_{\mathrm{LSQ}}(x_i) h'_{\mathrm{meso}}(x_i) \rangle = \sum_{k,k'=1}^{M} \sum_{j=1}^{N} Z^{-1}_{\mathrm{LSQ}_{k,k'}} F_k(x_i) F_{k'}(x_j) A_{ij}. \quad (18)$$

We thus have

$$\langle h'_{\mathrm{est}}(x_i)^2 \rangle = \langle [h(x_i) - \sum_{m=1}^{M} B_{\mathrm{LSQ}_m} F_m(x_i)]^2 \rangle = b^2 + \sigma^2(x_i) + \langle \epsilon_{\mathrm{LSQ}}(x_i)^2 \rangle - 2 \langle \epsilon_{\mathrm{LSQ}}(x_i) h'_{\mathrm{meso}}(x_i) \rangle. \quad (19)$$

Unauthenticated | Downloaded 10/04/22 03:28 AM UTC

b. Objective mapping by least-squares fitting (OM)

Objective mapping by least-squares fitting (Davis 1985) provides an estimate of the b_m by considering the noise statistics in the estimation of the orbit error. We need a nonbiased minimum variance estimator of the orbit error, which can be expressed in functional form (12). We obtain the following results (see Davis 1985 for the detailed calculations):

$$b_m = B_{\mathrm{OM}_m} = \sum_{k=1}^{M} \sum_{i,j=1}^{N} Z^{-1}_{\mathrm{OM}_{m,k}} F_k(x_i) h(x_j) A^{-1}_{ij} \quad (20)$$

where

$$Z_{\mathrm{OM}_{m,k}} = \sum_{i,j=1}^{N} F_m(x_i) F_k(x_j) A^{-1}_{ij}.$$

The covariance of the error on $B_{\mathrm{OM}_m}(\delta_{B\mathrm{OM}_m})$ is thus equal to

$$\langle \delta B_{\mathrm{OM}_m} \delta B_{\mathrm{OM}_n} \rangle = Z^{-1}_{\mathrm{OM}_{m,n}}. \quad (21)$$

The error on estimation of $\epsilon_{\mathrm{orb}}(x)\epsilon_{\mathrm{OM}}$ has now a variance given by

$$\langle \epsilon_{\mathrm{OM}}(x)^2 \rangle = \sum_{m,n=1}^{M} Z^{-1}_{\mathrm{OM}_{m,n}} F_m(x) F_n(x). \quad (22)$$

The correlation of this error with $h'_{\mathrm{meso}}(x_i)$ is

$$\langle \epsilon_{\mathrm{OM}}(x_i) h'_{\mathrm{meso}}(x_i) \rangle = \sum_{m,k=1}^{M} \sum_{j1,j2=1}^{N} Z^{-1}_{\mathrm{OM}_{m,k}} F_m(x_i) \times F_k(x_{j2}) A^{-1}_{j1j2} C(x_i, x_{j1}). \quad (23)$$

If $b = 0$ (i.e., zero altimetric noise or noise previously filtered), we have $\langle \epsilon_{\mathrm{OM}}(x_i) h'_{\mathrm{meso}}(x_i) \rangle = \langle \epsilon_{\mathrm{OM}}(x_i)^2 \rangle$. The variance after removing the long-wavelength part from the estimate is lower than the true variance in every case and is given by

$$\langle h'_{\mathrm{est}}(x_i)^2 \rangle = \langle [h(x_i) - \sum_{m=1}^{M} B_{\mathrm{OM}_m} F_m(x_i)]^2 \rangle = \sigma^2(x_i) - \langle \epsilon_{\mathrm{OM}}(x_i)^2 \rangle. \quad (24)$$

Although derived differently, this method is actually similar to the generalized weighted least-squares methods described by Liebelt (1967) and for noncorrelated, spatially uniform errors is equivalent to the conventional least squares method.

4. Application

First we shall apply these results to typical real situations at midlatitudes for homogeneous mesoscale variability. For first-degree polynomial adjustments, we consider arcs of 1500 km (e.g., Le Traon et al. 1990) and for second-degree adjustments, 2500-km arcs (e.g., Zlotnicki et al. 1989). The computed errors are compared to errors deduced from Cheney and Miller (1990) study. We compare them also to the corresponding polynomial modeling error for the orbit as estimated by Tai (1989) for different lengths of arcs (from 1500 to 10 000 km).

These results will then be applied to nonhomogeneous situations, i.e., cases where one track successively crosses regions of weak and strong mesoscale variability. First- and second-degree polynomial adjustments are investigated. Comparison is made with the results of Sandwell and Zhang (1989).

In these examples, the function used for spatial covariance of the mesoscale signal is that of Arhan and Colin de Verdière (1985):

$$C(r) = \sigma(x)\sigma(x+r) \times \left[1 + ar + \frac{1}{6}(ar)^2 - \frac{1}{6}(ar)^3\right] \exp(-ar). \quad (25)$$

Parameter a will be taken as 40 km^{-1} corresponding to a first zero crossing of C of 135 km. This is the scale typical of mesoscale variability at midlatitudes that can be obtained, for example, from Geosat data (Le Traon et al. 1990). The sensitivity of the results to the different correlation functions is discussed in the Appendix. For the sake of simplicity, we shall assume zero altimetric noise. The effect of altimetric noise on the errors studied is, in any case, much lower than mesoscale-induced error since it is a white noise.

a. Homogeneous variability

1) ADJUSTMENT BY A FIRST-DEGREE POLYNOMIAL OVER 1500 KM

We thus have two functions of $F_m(x)$ ($M = 2$, $F_1(x) = 1$, $F_2(x) = x$) and 150 data points on the profile ($N = 150$, sampling every 10 km). We consider a profile characterized by homogeneous mesoscale variability of 30 cm (rms), a typical value for western boundary currents.

The LSF method produces errors of 8 to 16 cm (see Fig. 1a). This error is given by a straight line, and its rms value has a functional shape of the $\sqrt{ax^2 + bx + c}$ (a and $c > 0$) type. It reaches a minimum at the center of the profile. The OM method produces slightly lower error (see Fig. 1a). The difference between the OM and LSF methods here lies solely in the fact that OM gives greater weight to the end points, which are more independent measures of the orbit error, as they have fewer neighbors. This is shown by the mesoscale signal rms variability curves (see Fig. 1b) once the polynomial has been subtracted: the error at the ends is relatively less correlated with the mesoscale signal when the LSF method is used, and the variability increases. However, with the OM method, the correlation between ϵ_{OM} and h'_{meso} is constant for all points.

Unauthenticated | Downloaded 10/04/22 03:28 AM UTC

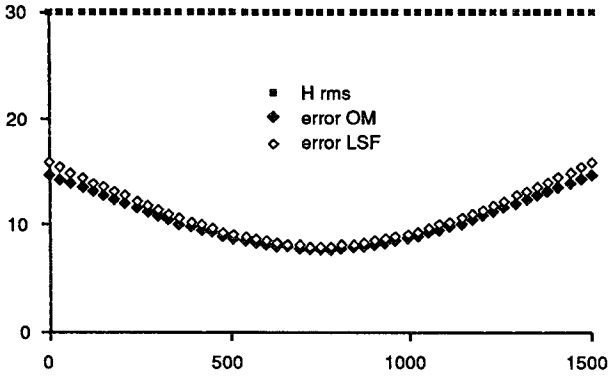

FIG. 1a. Root-mean-square error (cm) on altimetric heights due to removing a first-degree polynomial on a 1500-km profile. The variability of the mesoscale signal is assumed to be homogeneous and equal to 30 cm (rms). OM and LSF are the two methods of estimating the polynomial (see text).

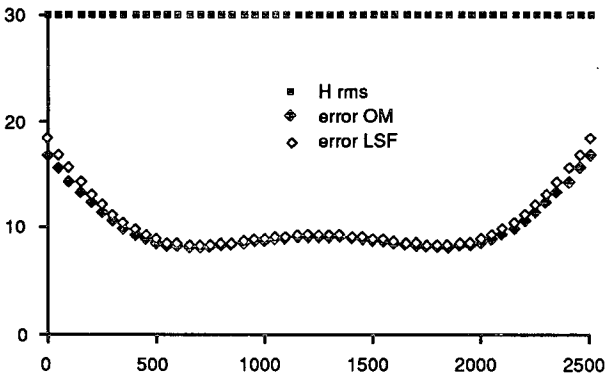

FIG. 2a. Root-mean-square error (cm) on the altimetric heights due to removal of a second-degree polynomial on a 2500-km profile. The signal variability is homogeneous and equal to 30 cm (rms).

2) ADJUSTMENT BY A SECOND-DEGREE POLYNOMIAL OVER 2500 KM

We now have three functions $F_m(x)$ ($M = 3$, $F_1(x) = 1$, $F_2(x) = x$, $F_3(x) = x^2$) and 250 data points on the profile. We still assume homogeneous mesoscale variability of 30 cm (rms). A second-degree polynomial fit provides similar results, though with slightly higher errors between 8 and 18 cm (although the arcs are longer) (Figs. 2a and 2b). The functional form is slightly more complex (square root of a fourth-degree polynomial).

3) INFLUENCE OF LEVEL OF MESOSCALE VARIABILITY

Similar results are obtained for weak variabilities, the rms errors being proportional to the rms mesoscale signal. Thus, for an rms mesoscale signal of 5 cm, the errors are only a sixth as high as in the above case (the relative errors are the same). Note, however, that with weak variabilities, the error due to altimetric noise, despite being lower (<0.5 cm for $b = 3$ cm), is relatively higher.

4) CHENEY AND MILLER (1990) STUDY

Cheney and Miller (1990) show that adjustment of a second-degree polynomial over distances of 2000–3000 km removes more than half of the total signal in the western tropical Pacific. The rms differences between Geosat and Ponape tide gauge measurements were thus as large as 5.6 cm for a total rms signal of around 8 cm. A crude estimate of decorrelation scales in these tropical regions is about 500 km. This corresponds to $a = 160$ km^{-1} and relative errors typically two times larger than in the previous examples. Since the signal is also approximately four times smaller that in the previous examples, this actually gives errors two times smaller. According to Fig. 2a (LSF method), this would mean rms error comprised between 4-cm rms (at the center of the profile) and 9-cm rms (at the ends) in good agreement with Cheney and Miller (1990) estimations. Using first-degree polynomial adjustment over a longer arc (more than 10 000 km),

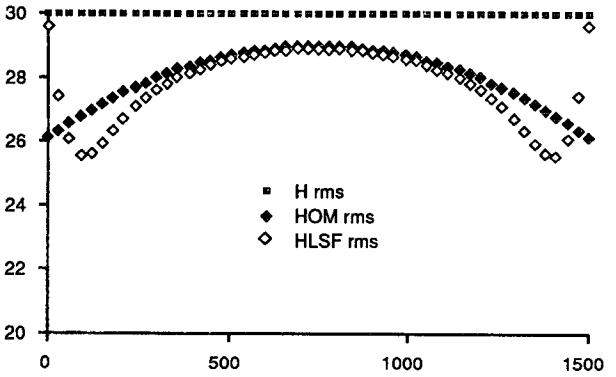

FIG. 1b. Root-mean-square variability (cm) of the altimetric height after the removal of the polynomial. Here HOM and HLSF represent the variability when the polynomial is adjusted by the OM and LSF methods, respectively.

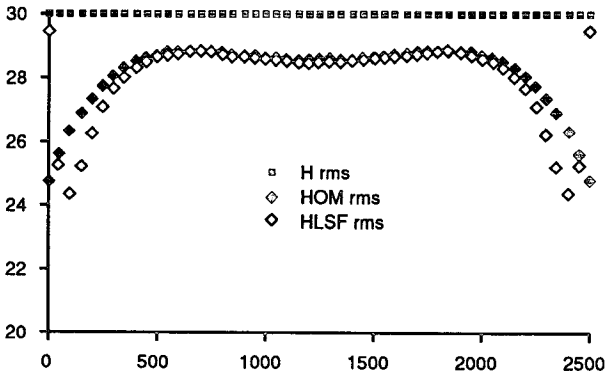

FIG. 2b. Root-mean-square variability (cm) of altimeter heights after removal of polynomial.

Unauthenticated | Downloaded 10/04/22 03:28 AM UTC

they were able to recover most of the signal. For such polynomial adjustment, our calculation would give rms errors of only 1.5 cm at the center of the profile and 3.1 cm at the ends. As Cheney and Miller (1990) were only interested in the central part of the profile, the induced errors were thus almost negligible. Note, however, that for this long arc adjustment, the polynomial modeling error for the orbit was no more negligible and was decreased afterwards by averaging.

5) Comparison with polynomial modeling error for the orbit

It is very useful to compare the adjustment error to polynomial modeling error for the orbit (i.e., the errors investigated by Tai 1989). Indeed, a sound choice of polynomial adjustment (arc length, degree of polynomial) should minimize the sum of these two errors. Note, however, that other errors, such as geophysical corrections residual errors, need also to be taken into account. There is clearly a trade-off between having a long-arc and/or a low-degree polynomial to minimize the errors induced by mesoscale variability and having, on the opposite, a short-arc and/or high-degree polynomial to minimize the orbit error modeling error. It can be examined theoretically given the mesoscale and orbit error statistical characteristics. As an illustration, Fig. 3 compares the rms errors (averaged on the arc) due to first- and second-degree polynomial adjustments (LSF method) to corresponding polynomial modeling errors for the orbit as estimated by Tai (1989) for different lengths of arcs (from 1500 km to 10 000 km). A homogeneous mesoscale signal of 15-cm rms (with the covariance model previously used) and a 1-m rms orbit error are assumed for this particular comparison (the errors for different rms mesoscale and orbit error signal are easily deduced by proportionality). In this case, for first-degree polynomial adjustments the modeling error dominates only for arc longer than 5000 km, while for second-degree polynomial the modeling error is always negligible compared to error due to polynomial adjustment. For this particular example, length arcs of 5000 km and 10 000 km, respectively, for first- and second-degree polynomial adjustments would minimize the sum of these two errors.

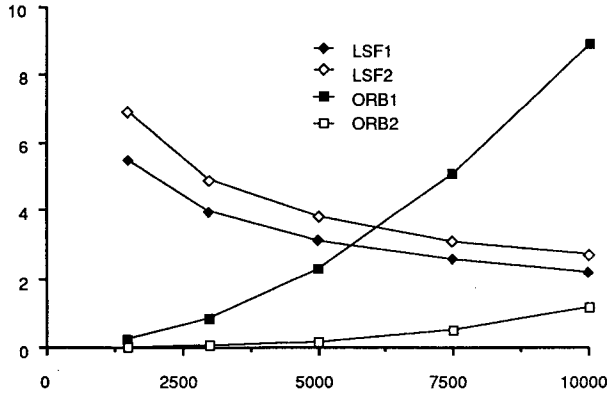

FIG. 3. Root-mean-square errors (averaged on the arc) due to first-degree (LSF1) and second-degree polynomial adjustments (LSF2) and corresponding orbit error modeling errors (ORB1 and ORB2) for different lengths of arcs. A homogeneous mesoscale signal of 15 cm rms and a 1-m rms orbit error are assumed.

b. *Nonhomogeneous variability*

1) Adjustment by a first-degree polynomial over 1500 km ($N = 150$) and a second-degree polynomial over 2500 km ($N = 250$)

Assume nonhomogeneous mesoscale variability, with profile variations of the following type (e.g., a track crossing the Gulf Stream):

$$\sigma(x_i) = 30 \text{ cm} \quad \left(i = 1, \cdots, \frac{N}{3}\right)$$

$$\sigma(x_i) = 30 - 25\,\frac{i - (N/3)}{(N/3)} \text{ cm} \times \left(i = \frac{N}{3} + 1, \cdots, 2\,\frac{N}{3}\right)$$

$$\sigma(x_i) = 5 \text{ cm} \quad \left(i = 2\,\frac{N}{3}, \cdots, N\right).$$

When the profile is adjusted by a first-degree polynomial, the LSF error (see Fig. 4a) is between 3 and 15 cm and is greater than the signal in the weak-variability region. The variabilities after removal of the polynomial are lower than the true variabilities in the high-variability area and greater in the weak-variability area. Too much weight is therefore given to the data in the high mesoscale variability area, this data being, by definition, noisier as far as estimation of the orbit error is concerned. The polynomial is too constrained by these data. The signal subtracted by the polynomial is therefore correlated with the mesoscale signal in that area (variability after removal is reduced) and noncorrelated in the weak-variability area (variability after removal is increased). The OM method produces noticeably less important errors (Fig. 4a) between 1.5 and 8 cm. The variabilities after removal of the polynomial (see Fig. 4b) are much closer to the true variabilities. The OM method gives around 36 (i.e., 30/5 squared) times more weight to the data in the area of weak variability than the conventional LSF method.

The results of second-degree adjustment are also shown in Figs. 5a and 5b. The errors are higher and have a more complex shape. Note that in relation to the first degree, under the LSF method, the second degree tends to "smooth" the front between the high variability and the weak variability areas. Here too, the OM method gives far better results.

Unauthenticated | Downloaded 10/04/22 03:28 AM UTC

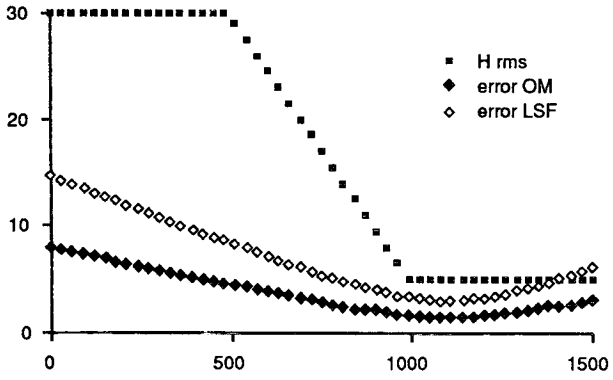

FIG. 4a. Root-mean-square error (cm) on altimeter heights due to removal of a first-degree polynomial on a 1500-km profile. The variability of the mesoscale signal is nonhomogeneous and varies between 30 and 5 cm (rms).

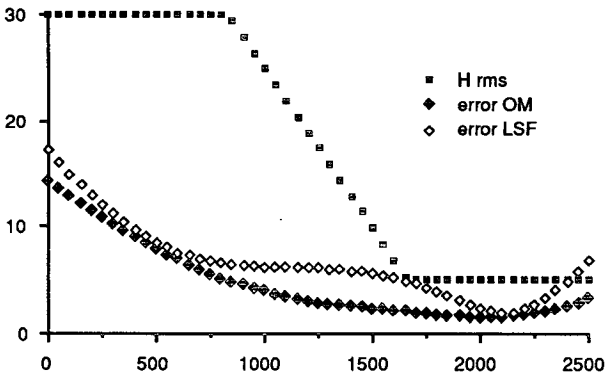

FIG. 5a. Root-mean-square error (in cm) on altimeter heights due to removal of second-degree polynomial on a 2500-km profile. The variability of the mesoscale signal is nonhomogeneous and varies between 30 and 5 cm (rms).

2) EXAMPLE OF SANDWELL AND ZHANG (1989)

Sandwell and Zhang (1989) analyzed Geosat data and showed that adjusting a bias and tilt in cases of nonhomogeneous mesoscale variability could cause significant artificial variabilities at the ends of the profiles. We shall resume the example that they studied experimentally and examine it from a theoretical point of view.

The Sandwell and Zhang arc is 3000 km long ($N = 300$). The variability shows roughly the variations depicted in Fig. 6a: two areas of weak variability at the edges and an area of high variability at the center. In this configuration, the error under the LSF method (see Fig. 6a) is between 4 and 6 cm. It is on the order of or greater than the signal at the ends. The variabilities (see Fig. 6b) once the polynomial has been subtracted are higher than the true variabilities at the ends and lower at the center of the profile, for the same reason as in the case studied above. This was exactly what Sandwell and Zhang (1989) observed from Geosat data. Our theoretical analysis shows, quantitatively, the error introduced by adjusting the polynomial. Note, again, that the OM method produces considerably less error, and that the variability after the polynomial has been subtracted is much closer to the true variability (see Figs. 6a and 6b).

5. Verification of results from simulated and real data

a. Simulated data

We used simulated data to verify certain of the theoretical results discussed in section 4. A unidimensional field of dynamic height was generated along a track $D(x_i)$, $i = 1, \cdots, 150$ with a sampling interval of 10 km, using a pseudorandom Gaussian vector generator. The field is fully determined by the mean value $\langle D(x) \rangle$ at each point (zero in our case) and the covariances $\langle D(x_1)D(x_2) \rangle$ for all pairs x_1, x_2. These were obtained from the model mentioned above. Two simulations were done: simulation A, for homogeneous mesoscale variability, and simulation B, for nonhomogeneous mesoscale variability. In both cases, 10 000 realizations were generated. This provides statistical accuracy on rms variabilities lower than 1%.

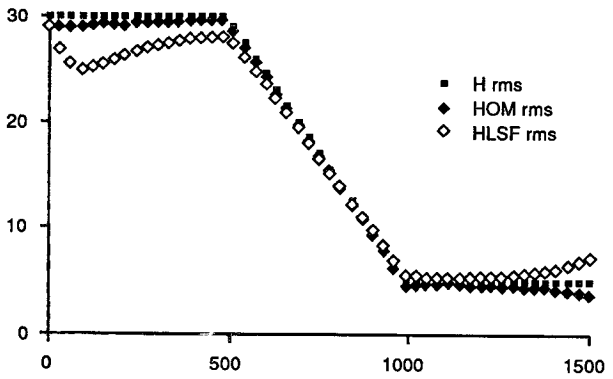

FIG. 4b. Root-mean-square variability (cm) of altimeter heights after removal of polynomial.

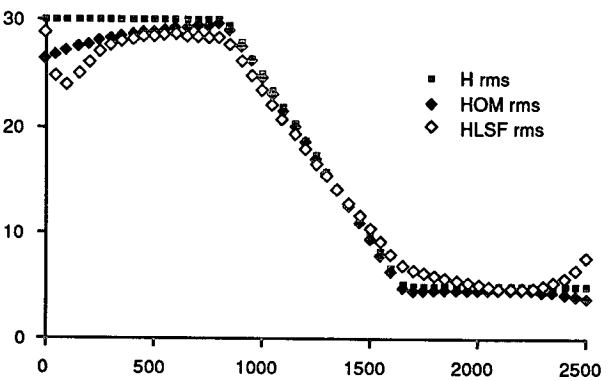

FIG. 5b. Root-mean-square variability (cm) of altimeter heights after removal of a polynomial.

Unauthenticated | Downloaded 10/04/22 03:28 AM UTC

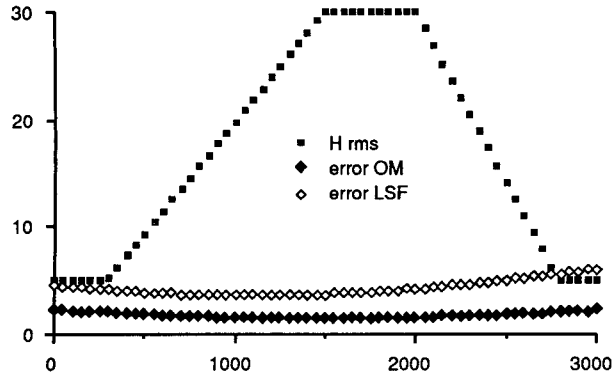

FIG. 6a. Root-mean-square error (cm) on altimeter heights due to the removal of a first-degree polynomial on a 3000-km profile. The variability of the mesoscale signal is nonhomogeneous and varies between 30 cm and 5 cm (rms). It corresponds to the signal in the case studied by Sandwell and Zhang (1989).

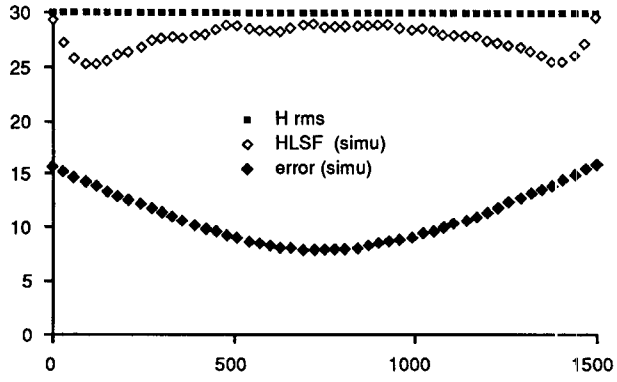

FIG. 7. Simulation of error related to the removal of a first-degree polynomial over 1500 km by LSF method and its effect on mesoscale signal variability (simulation A).

For simulation A, we chose homogeneous mesoscale variability with an amplitude (rms) of 30 cm. For each realization of the fit, we subtracted a first-degree polynomial and estimated the error due to subtracting it. Figure 7 shows the rms mesoscale variability after removal of the polynomial, plus the rms error due to subtracting it. As expected, the two agree entirely with the theoretical estimates given in Figs. 1a and 1b.

For simulation B we tested our results, using the LSF and OM methods, for nonhomogeneous variability. We simulated a mesoscale field with a variability profile the same as that given in Fig. 4a. The OM method, if applied as described in section 3b, requires the inversion of an $N \times N$ matrix, which is more penalizing in time than the LSF method. However, in practice, looser sampling can be done, or the data initially averaged out. The method can also be used in a degraded mode, assuming the decorrelation of measurements from one point to the next and weighting only by the inverse of the variability squared (i.e., diagonal matrix **A**). This is the method used for our simulation.

Figure 8 shows that the errors in the degraded OM method are only slightly higher than in the OM method (10 cm at the ends instead of 8 cm); these results can, of course, be obtained theoretically. Figure 8 also shows the theoretical results of Figs. 5a and 5b for the LSF method.

b. Real data

To compare the theoretical results discussed in section 4 with real data, we selected 4 consecutive ascending Geosat tracks over 56 cycles in the northwest Atlantic. The tracks are between 10° and 35°N, 70° and 60°W and cross areas of relatively homogeneous variability. They make up a set of 178 altimeter profiles (46 profiles are missing or incomplete). Assuming the four tracks to be independent, and decorrelation of one cycle in every two, we have roughly 100 degrees of freedom and statistical accuracy on the rms variability estimate better than 10%. The maximum length of the tracks is 2700 km. Sea surface height profiles were first resampled every 10 km using a cubic spline

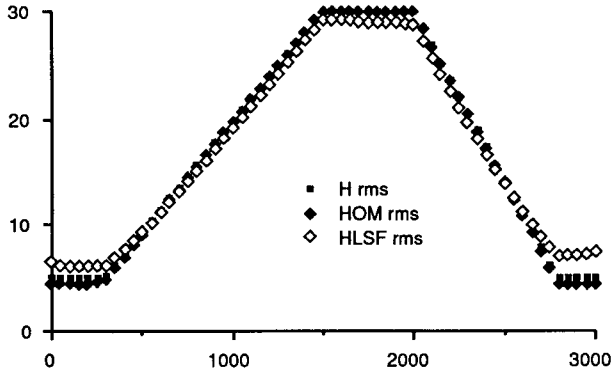

FIG. 6b. Root-mean-square variability (cm) of altimeter heights after removal of a polynomial.

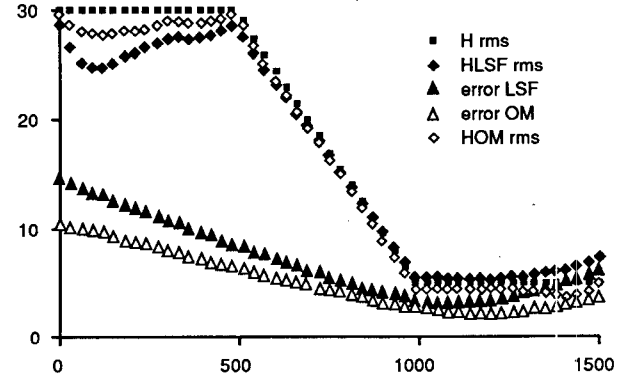

FIG. 8. Same as Fig. 7 but for nonhomogeneous mesoscale variability and for both LSF and OM methods (simulation B). The OM method is applied in a degraded mode (see text).

Unauthenticated | Downloaded 10/04/22 03:28 AM UTC

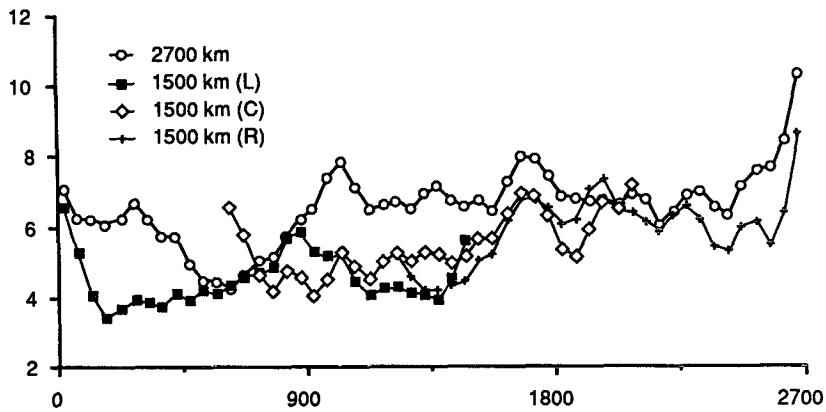

FIG. 9. Root-mean-square mesoscale variability on 178 Geosat profiles in the northwest Atlantic. Profile length is 2700 km. The four curves represent the variabilities after removal of a first-degree polynomial over 2700 km and over three 1500-km portions of the profile: left (L), center (C), and right (R).

to provide regular sampling. Then, for each profile, we subtracted the mean profile and applied a Lanczos filter with a cutoff wavelength of 100 km to reduce the altimeter noise. Conventional bias and tilt adjustment (LSF method) was done on the entire 2700-km profiles so obtained to provide a reference base. Three other types of bias and tilt adjustment (LSF method) over 1500 km were done, one on the first 1500 km (L), one centered on 600 to 2100 km (C), and one on the last 1500 km (R).

The characteristics suggested by theory are found in the rms variabilities obtained after these different adjustments (see Fig. 9), namely variability lower at the center of the profile and rising at the edges (e.g., L profiles). This particularly applies to comparison of the 1500-km profile variabilities (L, C, R) with that of the 2700-km profile. This is also borne out by comparison of the variabilities of the three 1500-km profiles (L, C, R) in the overlap area (at the center); the variabilities of the L and R profiles rise more than that of the C profile at the edges. For track C, the variability at the far left is in fact greater than that of the 2700-km profile. This is due to the nonhomogeneity of the mesoscale variability on that particular track and the influence of the more energetic right-hand part of profile C. Such behavior is similar to the theoretical behavior shown in Fig. 4b.

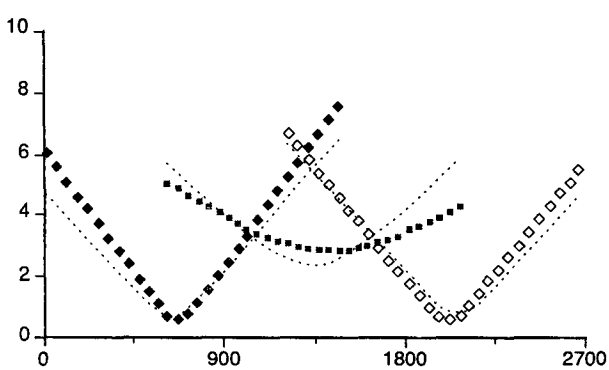

FIG. 10. Root-mean-square differences between altimeter residuals of the three 1500-km profiles and those of the 3000-km profile. The dotted lines show the theoretical relative errors obtained using the results of section 3.

A more quantitative comparison was done by comparing the relative errors observed $e_{r_{obs}}$ [$e_{r_{obs}}$ = (residuals on 1500-km profiles − residuals on 2700-km profiles)] to e_r, the theoretical relative errors. Indeed, e_r is equal to $(e_1 - e_2)$, e_1 being the adjustment error on the 1500-km profiles and e_2 the error on the 2700-km profile.

Here $\langle e_r^2 \rangle$ is easily obtained for the different 1500-km profiles (L, C, R) in accordance with the results of section 3:

$$\langle e_r(x)^2 \rangle = \sum_{m,n,k,k'=1}^{M} \sum_{i,j=1}^{270} Z^{-1}_{\mathrm{LSQ12}_{m,k,i}} Z^{-1}_{\mathrm{LSQ12}_{n,k',j}} \times F_k(x_i) F_{k'}(x_j) A_{ij} F_m(x) F_n(x) \quad (26)$$

where

$$Z^{-1}_{\mathrm{LSQ12}_{m,k,i}} = \begin{cases} Z^{-1}_{\mathrm{LSQ1}_{m,k}} - Z^{-1}_{\mathrm{LSQ2}_{m,k}}, & \text{when } i \text{ belongs to 1500-km profile} \\ -Z^{-1}_{\mathrm{LSQ2}_{m,k}}, & \text{when } i \text{ does not belong to 1500-km profile.} \end{cases}$$

$Z_{\mathrm{LSQ2}_{m,k}} = \sum_{i=1}^{270} F_m(x_i) F_k(x_i)$ and $Z_{\mathrm{LSQ1}_{m,k}} = \sum_{i=1}^{150} F_m(x_i) F_k(x_i)$ (L profile), $\sum_{i=61}^{210} F_m(x_i) F_k(x_i)$ (C profile), $\sum_{i=121}^{270} F_m(x_i) F_k(x_i)$ (R profile).

Figure 10 shows the theoretical relative errors $\langle e_r(x)^2 \rangle^{1/2}$ computed for the three 1500-km profiles (L, C, R), shown as dotted lines, overlaid on the true observed errors $\langle e_{r_{obs}}(x)^2 \rangle^{1/2}$. Before the calculation,

Unauthenticated | Downloaded 10/04/22 03:28 AM UTC

we estimated the mean spatial autocorrelation function from the residuals of all the 2700-km profiles. This has a zero crossing at around 400 km. To achieve a realistic estimate of the errors, these were therefore calculated using the covariance model mentioned above, but this time with a parameter a^{-1} of 120 km (instead of 40 km). The mesoscale variability was assumed to be homogeneous and to have a rms amplitude equal to 8 cm. Given the assumptions concerning the autocorrelation function and homogeneity and the statistical precision, the agreement between the theoretical and the real values is excellent. Also note that we assumed that the adjustment over 2700 km truly removes all orbit error, while in fact it probably leaves orbit error on the order of a few centimeters rms with the Geosat GDR data (Tai 1989).

6. Comparison with objective analysis

Before concluding, it is useful to compare these least squares methods with optimal signal estimation methods such as objective analysis (Bretherton et al. 1976). For example, orbit error could be estimated by taking account not only of its spatial characteristics (as above) but also its energetic characteristics (variance). The fact is that the above methods adjust a long-wavelength signal even if, for example, the orbit error is zero or has very low variance. Objective analysis takes account of all the signal and noise statistics. The optimal estimation, $\epsilon_{\text{orb\_est}}$, of the orbit error, ϵ_{orb}, is given by the linear combination of the $h(x_i)[h(x_i) = \epsilon_{\text{orb}}(x_i) + h'_{\text{meso}}(x_i)]$ data that minimizes the error $\langle(\epsilon_{\text{orb\_est}} - \epsilon_{\text{orb}})^2\rangle$. We thus obtain (Bretherton et al. 1976):

$$\epsilon_{\text{orb\_est}}(x) = \sum_{i,j=1}^{N} C_{xi} A_{ij}^{-1} h(x_i). \quad (16)$$

The error $\langle e(x)^2\rangle$ on the estimation is expressed as follows:

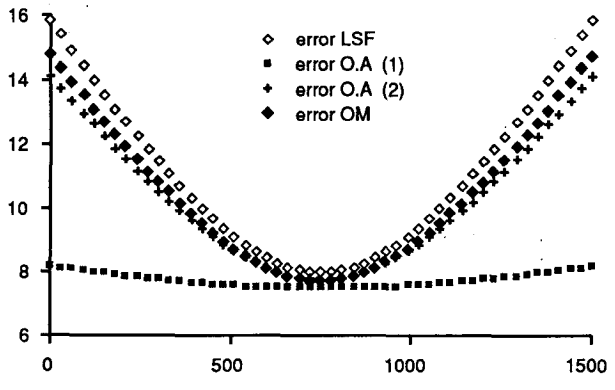

FIG. 11. Comparison of errors on estimation of orbit error using different methods. LSF and OM are the polynomial adjustment methods described in the paper. OA(1) and OA(2) are the objective analysis methods for variances of orbit error of $(30\text{ cm})^2$ and $(1\text{ m})^2$ respectively.

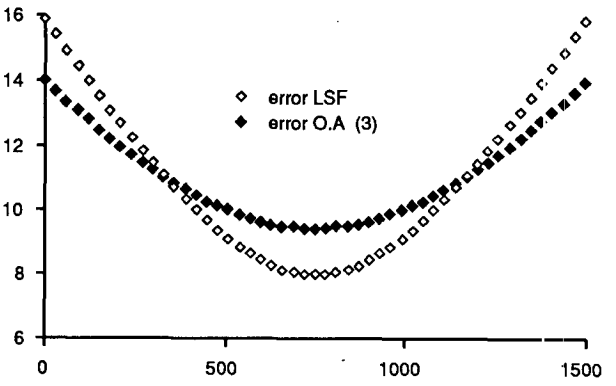

FIG. 12. Comparison of errors on estimation of orbit error by LSF method and by objective analysis, if variance of orbit error is underestimated as $(30\text{ cm})^2$ instead of $(1\text{ m})^2$ [OA(3)].

$$\langle e(x)^2\rangle = \langle \epsilon_{\text{orb}}(x)^2\rangle - \sum_{r,s=1}^{N} C_{xr} C_{xs} A_{rs}^{-1} \quad (17)$$

where

$$A_{ij} = \langle h(x_i)h(x_j)\rangle = \langle \epsilon_{\text{orb}}(x_i)\epsilon_{\text{orb}}(x_j)\rangle + \langle h'_{\text{meso}}(x_i)h'_{\text{meso}}(x_j)\rangle$$

$$C_{xi} = \langle \epsilon_{\text{orb}}(x)h(x_i)\rangle = \langle \epsilon_{\text{orb}}(x)\epsilon_{\text{orb}}(x_i)\rangle$$

(mesoscale signal noncorrelated with orbit error).

When orbit error is estimated for a profile from data generated for that specific profile, only the spatial data is used, and the covariance of the orbit error can be approximated by

$$\langle \epsilon_{\text{orb}}(x_i)\epsilon_{\text{orb}}(x_j)\rangle = \langle \epsilon_{\text{orb}}^2\rangle \cos\frac{2\Pi|x_i - x_j|}{40\,000}$$

(x_i in km) (e.g., Wunsch and Zlotnicki 1984).

Figure 11 shows the error obtained on a 1500-km arc for different variances of the orbit error $(30\text{ cm})^2$ [method OA (1)] or $(1\text{ m})^2$ [method OA (2)] and a mesoscale variance of $(30\text{ cm})^2$. As objective analysis is an optimal method, the error is always lower than that obtained previously by the least-squares methods (LSF and OM for a first-degree polynomial adjustment). With a 30-cm rms orbit error, the error is practically uniform and on the order of 8 cm. When the orbit variance is significant relative to mesoscale variance, objective analysis and the LSF and OM methods produce comparable errors. Objective analysis methods are therefore useful for low orbit errors but, unlike adjustment, require accurate orbit error statistics. If these statistics are not sufficiently accurately known, such methods are no longer optimal, as the next example shows. We calculated the error obtained when underestimating the orbit error (30 cm rms instead of 1 m rms). In such a case, Fig. 12 shows that the objective analysis error [OA (3)] is greater than that for the LSF method at the center of the profile. Objective analysis

Unauthenticated | Downloaded 10/04/22 03:28 AM UTC

also requires inversion of an $N \times N$ matrix, and should only be used if there is an appreciable benefit.

7. Summary and conclusion

Though the oceanic mesoscale signal and the altimetric orbit error signal have very different spatial scales, the polynomial adjustment technique used to eliminate the orbit error is known to affect the mesoscale signal. A theoretical study of that problem was presented here. The fact is that polynomial adjustment subtracts part of the mesoscale signal of interest, since there is insufficient independent data (degrees of freedom) along the profile to constrain estimation of the polynomial satisfactorily. The signal subtracted differs from one profile to another and from one track to the next, which can pose problems for two-dimensional (x, y) or three-dimensional (x, y, t) mapping of altimetric heights.

The error due to these polynomial adjustments is, obviously, dependent on the spatial and energetic characteristics of the mesoscale signal. We calculated it theoretically for values typical of midlatitude regions. In cases of homogeneous mesoscale variability, its amplitude is typically between 30% (at the center of the profile) and 50% (at the edges) of the total mesoscale signal for a first-degree fit over 1500 km or a second-degree fit over 2500 km. The error is, of course, correlated with the mesoscale signal, and the rms variability after removing the polynomial is always lower than the true variability. In nonhomogeneous cases, the error can be greater than the mesoscale signal. We have shown that more efficient least-squares methods that take account of the mesoscale statistics can be extremely useful, particularly for areas of strong nonhomogeneity. Errors can thus be halved. These methods are also easy to implement given an a priori knowledge of the mesoscale variability. Our results have been checked using simulated data and validated against real Geosat data.

This work clearly quantifies and demonstrates the effects of these polynomial adjustments on the mesoscale signal of interest. In our opinion, this type of analysis is needed to make a sound choice of polynomial adjustment (arc length, degree of polynomial) given the mesoscale signal and orbit error characteristics. The adjustment must not, therefore, be chosen solely according to whether it accurately represents the orbit error but also—especially—according to the accuracy with which it can be estimated. It can thus be preferable to remove less of the ocean signal, even if it means obtaining a less accurate representation of the orbit error. Anyway, as the induced errors are nonnegligible, they should be taken into account when interpreting or using the data obtained, for example when the data is input to models.

The polynomial adjustment methods and objective analysis described in this study use only along-track, instantaneous spatial information. Through more complex methods using cross-track information, estimations of the orbit error could be considerably better constrained (e.g., Tai 1988). More generally, using inverse techniques the orbit error signal could be obtained through a global adjustment taking account not only the spatial but also the temporal characteristics of the signal and of the noise. Work is currently in progress to show the contribution of such inverse methods that will eventually provide a better means of extracting the mesoscale signal.

Acknowledgments: Geosat data were processed at GRGS/CNES (Groupe de Recherche en Géodésie Spatiale). This study was supported by a SHOM/GERDSM/CLS ARGOS Contract A 89 48 648 00.

APPENDIX

Influence of Mesoscale Spatial Autocorrelation Function on Estimation of Errors Due to Polynomial Adjustment

a. Parameter a

Parameter a of the Arhan and Colin de Verdière (1985) autocorrelation function (25) used in this paper determines the spatial scale of eddies. Since the spatial scale of eddies increase with a^{-1}, errors will, naturally, increase with a^{-1} as it is more difficult to distinguish between the mesoscale signal and the orbit error signal. The number of degrees of freedom NL (approximately the number of independent estimates) is linked to the integral scale IS,

$$\mathrm{IS} = \int_{-\infty}^{\infty} C(r)/C(0)\,dr \tag{A1}$$

by

$$\mathrm{NL} = L/\mathrm{IS} \tag{A2}$$

where L is the profile length.

The rms errors are a priori expected to vary approximately with $\sqrt{\mathrm{IS}/L}$. For example, the rms error on estimation of a mean or bias can be approximated by $\sigma\sqrt{\mathrm{IS}/L}$ (Flierl and McWilliams 1977). As IS is proportional to a^{-1} (IS = $8/3a$ for the above function), the rms errors are approximately proportional to $\sqrt{a^{-1}}$.

b. Shape of function

The shape of the function also influences the errors once the polynomial has been subtracted. Thus, by choosing the $C(r)$ function used by De Mey and Robinson (1987), hereafter denoted DMR function),

$$C(r) = \sigma(x)\sigma(x+r)\left[1 + ar - \frac{1}{3}(ar)^3\right]\exp(-ar) \tag{A3}$$

Unauthenticated | Downloaded 10/04/22 03:28 AM UTC

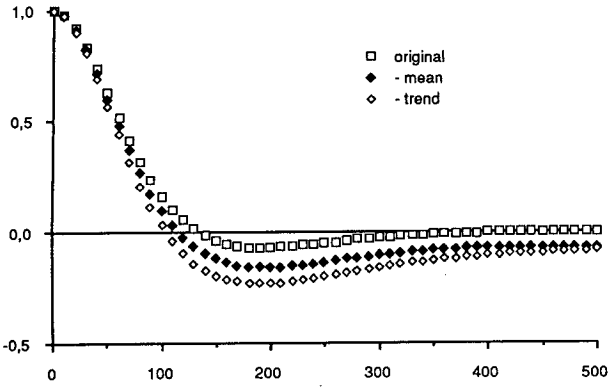

FIG. A1. Simulation of effect of removing a bias and removing a bias and tilt on the mesoscale signal spatial autocorrelation function.

with equivalent spatial scales (first zero crossing at around 120 km, i.e., $a = 60$ km^{-1}), the errors would have been roughly halved (4 cm at the center and 11 cm at the edges in Fig. 1b). This function has a large negative lobe and its integral scale is zero. This explains the lower errors (more independent estimates). In addition, the kinetic energy spectrum for this function is zero, or even slightly negative, at long wavelengths (larger than $15.4a^{-1}$, that is roughly larger than 1000 km). This has little physical meaning but appears to be characteristic of the altimeter-derived mesoscale signal after removal of a bias and tilt (e.g., Le Traon et al. 1990). We therefore advance the idea that the large negative lobes of altimetric autocorrelation functions are mostly due to the tilt and bias adjustment.

To show this, we calculated the spatial autocorrelation function $C(r)$ after removing a bias and a bias and tilt using the data in simulation A (section 4). Figure A1 shows the $C(r)$ function before removal [Arhan and Colin de Verdière (1985) model], after removing a bias and after removing a bias and tilt. The $C(r)$ functions have significant negative lobes after removal of the polynomial. Clearly, the result will depend on the shape of the initial function (before removal). In particular, if it already has a significant negative lobe, it will be less affected.

REFERENCES

Arhan, M., and A. Colin de Verdière, 1985: Dynamics of eddy motions in the eastern North Atlantic. *J. Phys. Oceanogr.*, **15,** 153–170.

Bretherton, F. P., R. E. Davis and C. B. Fandry, 1976: A technique for objective analysis design of oceanographic experiments applied to Mode 73. *Deep-Sea Res.*, **23,** 559–582.

Cheney, R. E., and L. Miller, 1990: Recovery of sea level signal in the western tropical Pacific from Geosat altimetry. *J. Geophys. Res.*, **95,** 2977–2984.

——, J. G. Marsh and B. D. Beckley, 1983: Global mesoscale variability from collinear tracks of Seasat altimeter data. *J. Geophys. Res.*, **88,** 4343–4354.

Davis, R. E., 1985: Objective mapping by least square fitting. *J. Geophys. Res.*, **90,** 4773–4777.

De Mey, P., and A. R. Robinson, 1987: Assimilation of altimeter eddy fields in a limited area quasi-geostrophic model. *J. Phys. Oceanogr.*, **17,** 2280–2293.

Flierl, G. R., and J. C. McWilliams, 1977: On the sampling requirements for measuring moments of eddy variability. *J. Mar. Res.*, **35,** 797–820.

Jourdan, D., 1990: Observation des structures océaniques par altimétric satellitaire: Influence des corrections d'environnement sur la restitution du signal mésoéchelle, Thèse de doctorat de P'Université Paul Sabatier, 171 pp.

Le Traon, P. Y., M. C. Rouquet and C. Boissier, 1990: Spatial scales of mesoscale variability in the North Atlantic as deduced from GEOSAT data. *J. Geophys. Res.*, **95,** 20 267–20 285.

Liebelt, P. B., 1967: *An Introduction to Optimal Estimation.* Addison–Wesley, 273 pp.

Rosborough, G. W., and J. A. Marshall, 1990: Effect of orbit error on determining sea surface variability using satellite altimetry. *J. Geophys. Res.*, **95,** 5273–5277.

Sandwell, D. T., and B. Zhang, 1989: Global mesoscale variability from the GEOSAT exact repeat mission: Correlation with ocean depth. *J. Geophys. Res.*, **94**(C12), 17 971–17 984.

Tai, C. K., 1988: GEOSAT crossover analysis in the tropical Pacific. Part I: Constrained sinusoidal crossover adjustment. *J. Geophys. Res.*, **93,** 10 621–10 629.

——, 1989: Accuracy assessment of widely used orbit error approximations in satellite altimetry. *J. Atmos. Ocean. Technol.*, **6,** 147–150.

Wunsch, C., and V. Zlotnicki, 1984: The accuracy of altimetric surfaces. *Geophys. J. Roy. Astr. Soc.*, **78,** 795–808.

Zlotnicki, V., L. L. Fu and W. Patzert, 1989: Seasonal variability in global sea level observed with GEOSAT altimetry. *J. Geophys. Res.*, **94,** 17 959–17 969.

Unauthenticated | Downloaded 10/04/22 03:28 AM UTC